First-Principles Study of the Honeycomb-Lattice Iridates Na_2IrO_3 in the Presence of Strong Spin-Orbit Interaction and Electron Correlations

Youhei Yamaji, Yusuke Nomura, Moyuru Kurita, Ryotaro Arita, and Masatoshi Imada
Department of Applied Physics, University of Tokyo, Hongo, Bunkyo-ku, Tokyo, 113-8656, Japan
(Received 21 January 2014; revised manuscript received 3 July 2014; published 2 September 2014)

An effective low-energy Hamiltonian of itinerant electrons for iridium oxide Na_2IrO_3 is derived by an *ab initio* downfolding scheme. The model is then reduced to an effective spin model on a honeycomb lattice by the strong coupling expansion. Here we show that the *ab initio* model contains spin-spin anisotropic exchange terms in addition to the extensively studied Kitaev and Heisenberg exchange interactions, and allows us to describe the experimentally observed zigzag magnetic order, interpreted as the state stabilized by the antiferromagnetic coupling of the ferromagnetic chains. We clarify possible routes to realize quantum spin liquids from existing Na_2IrO_3.

DOI: 10.1103/PhysRevLett.113.107201 PACS numbers: 75.10.Jm, 71.15.−m, 75.10.Kt

Introduction.—Cooperation and competition between strong electron correlations and spin-orbit couplings have recently attracted much attention. Iridium oxides offer a playground for such an interplay and indeed exhibit intriguing rich phenomena [1–4].

Especially, a theoretical prediction [1,2] on the possible realization of quantum spin liquid state and Majorana fermion state proven by Kitaev [5] as the ground state of an exactly solvable model now called the Kitaev model has inspired extensive studies on A_2IrO_3 (A = Na or Li) as a model system to realize the Kitaev spin liquid. However, although Na_2IrO_3 is an insulator (presumably a Mott insulator) with the optical gap ∼0.35 eV [6], it was shown that Na_2IrO_3 does not show spin liquid properties experimentally but exhibits a zigzag type magnetic order [7,8].

The Kitaev-Heisenberg model on the honeycomb lattice [1,2,9–11] was further proposed to describe Na_2IrO_3, which includes isotropic superexchange couplings in addition to the Kitaev-type anisotropic nearest-neighbor Ising interactions whose anisotropy axes depend on the bond directions. However, it turned out that this model cannot be straightforwardly consistent with the zigzag order either. This discrepancy inspired further studies on suitable low-energy effective Hamiltonians for A_2IrO_3 with A = Na or Li. First, models with further neighbor couplings [7,8,12,13] were studied. Additional Ising anisotropy [14] due to a strong trigonal distortion, which actually contradicts the distortions in the experiments [8] and in the *ab initio* treatments, was also examined. Quasimolecular orbitals [15], instead of the atomic orbitals assumed in the Kitaev-Heisenberg model, were claimed as a proper choice of the starting point. So far the origin of the zigzag type antiferromagnetic order observed for Na_2IrO_3 and the possible route to realize the quantum spin liquid are controversial.

In this Letter, we derive an *ab initio* spin model for Na_2IrO_3 and show that trigonal distortions present in Na_2IrO_3 in addition to the spin-orbit couplings hold the key: The simplest and realistic spin model for A_2IrO_3 will turn out to modify the Kitaev-Heisenberg Hamiltonian by additional anisotropic couplings as

$$\hat{H} = \sum_{\Gamma=X,Y,Z} \sum_{\langle \ell, m\rangle \in \Gamma} \vec{\hat{S}}_\ell^{\,T} \mathcal{J}_\Gamma \vec{\hat{S}}_m, \tag{1}$$

where $\vec{\hat{S}}_\ell^{\,T} = (\hat{S}_\ell^x, \hat{S}_\ell^y, \hat{S}_\ell^z)$ is a vector of SU(2) spin operators. The exchange couplings are given in matrices $\mathcal{J}_\Gamma$. The summations are over the nearest-neighbor pairs $\langle \ell, m\rangle$. The group of bond Γ with $\Gamma = X, Y$, and Z is defined in Fig. 1. The exchange matrices are parametrized as

$$\mathcal{J}_Z = \begin{bmatrix} J & I_1 & I_2 \\ I_1 & J & I_2 \\ I_2 & I_2 & K \end{bmatrix}, \qquad \mathcal{J}_X = \begin{bmatrix} K' & I_2'' & I_2' \\ I_2'' & J'' & I_1' \\ I_2' & I_1' & J' \end{bmatrix},$$
$$\mathcal{J}_Y = \begin{bmatrix} J'' & I_2'' & I_1' \\ I_2'' & K' & I_2' \\ I_1' & I_2' & J' \end{bmatrix}, \tag{2}$$

where we choose a real and symmetric parametrization by using U(1) and SU(2) symmetry of electron wave functions and spin operators, respectively. The details of these exchange parameters are described in the following discussion.

In addition to the Kitaev coupling K and K', and XY-type exchange J, magnetic anisotropy induced by a combination of spin-orbit couplings and trigonal distortions appears as anisotropic couplings such as I_1 and I_2. Here we note that our parametrization of the Kitaev term is different from that of Refs. [1,2,11]: The Kitaev term K in the present Letter corresponds to $-|K| + J$ in Refs. [1,2,11]. These anisotropic couplings drastically change candidate quantum phases and competition among them in Na_2IrO_3 and related materials. With these extensions, we show that the model allows a realistic description of Na_2IrO_3 and provides a basis for further search of quantum spin liquids. To achieve

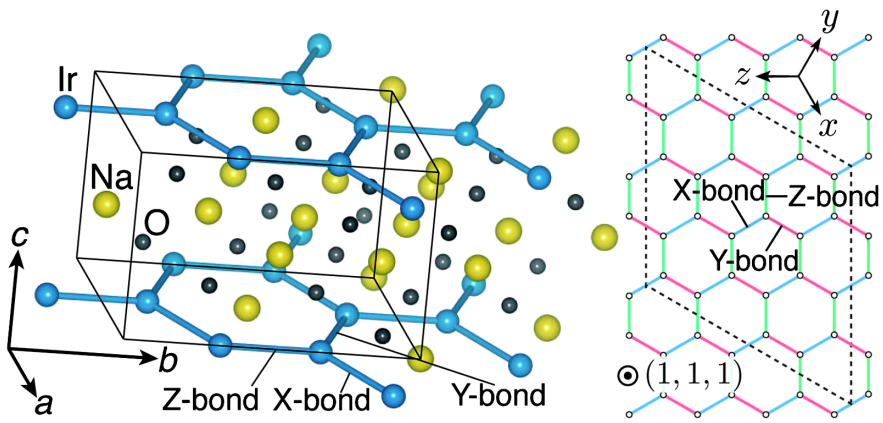

FIG. 1 (color online). Left panel: Crystal structure of Na_2IrO_3. Right panel: Honeycomb lattice with X, Y, and Z bonds. Same colored bonds indicate the same group. The x, y, and z axes in defining the t_{2g} orbitals are illustrated as directions out of the honeycomb plane. The honeycomb plane is then perpendicular to $(x, y, z) = (1, 1, 1)$. The dashed boundary represents a 24-site cluster used later for the exact diagonalization.

quantitative accuracy, we include the further neighbor couplings in our numerical calculations as detailed later.

Ab initio derivation and estimate of itinerant effective Hamiltonian.—To discuss the low-energy physics of Na_2IrO_3, we employ a recently proposed multiscale *ab initio* scheme for correlated electrons (MACE) [16]: First, we obtain the global band structure using the density functional theory (DFT). Second, using a Wannier projection on the Ir $5d$ t_{2g} target bands, we derive an effective model for the Ir $5d$ t_{2g} orbitals by the downfolding procedure taking into account the renormalization from the states other than the Ir $5d$ t_{2g} orbitals.

The global electronic structure was obtained by performing the density functional calculations using the Elk full-potential linearized augmented plane-wave code [17] with the Perdew-Wang exchange-correlation functional [18]. The resultant electronic structures agree with the previous DFT results [15] (see Supplemental Material [19]). We next constructed the Wannier orbitals from the Ir t_{2g} bands following the same procedure described in Ref. [20]. One-body parameters $t^{\sigma,\sigma'}_{\ell,m;a,b}$ in the low-energy Hamiltonian are given by the matrix elements of the Wannier orbitals as

$$t^{\sigma,\sigma'}_{\ell,m;a,b} = \int d\mathbf{r}_1 w^*_{\ell a\sigma}(\mathbf{r}_1)\hat{H}_{\mathrm{KS}} w_{mb\sigma'}(\mathbf{r}_1), \tag{3}$$

with the Kohn-Sham Hamiltonian $\hat{H}_{\mathrm{KS}}$ and the indices for sites ℓ and m, orbitals a and b, and spins σ and σ'.

The effective Coulomb interactions between these orbitals are estimated by the constrained random phase approximation (cRPA) [21]. Using the density response code for Elk [22], we obtain the *constrained* susceptibility of the noninteracting Kohn-Sham electrons $\chi_0(\mathbf{r}, \mathbf{r}', \omega)$ where contribution of particle-hole excitations within the target t_{2g} bands is excluded. We then calculate the partially screened Coulomb interaction

$$W(\mathbf{r}, \mathbf{r}', \omega) = \frac{1}{|\mathbf{r}-\mathbf{r}'|} + \int d\mathbf{r}_1 d\mathbf{r}_2 \frac{\chi_0(\mathbf{r}_1, \mathbf{r}_2, \omega)}{|\mathbf{r}-\mathbf{r}_1|} W(\mathbf{r}_2, \mathbf{r}', \omega),$$

which yields the Coulomb interaction between the Wannier orbitals w as

$$U_{\mathcal{KLMN}} = \lim_{\omega\to 0} \int d\mathbf{r}_1 d\mathbf{r}_2 w^*_{\mathcal{K}}(\mathbf{r}_1) w^*_{\mathcal{L}}(\mathbf{r}_2) W(\mathbf{r}_1, \mathbf{r}_2, \omega) \times w_{\mathcal{M}}(\mathbf{r}_1) w_{\mathcal{N}}(\mathbf{r}_2),$$

where $\mathcal{K}$, $\mathcal{L}$, $\mathcal{M}$, and $\mathcal{N}$ are the combined indices for the orbital and site.

Ab initio model for t_{2g} Hamiltonian.—The derived multiband model consisting of a t_{2g} manifold of the iridium atoms is given by the t_{2g}-Hamiltonian

$$\hat{H}_{t2g} = \hat{H}_0 + \hat{H}_{\mathrm{tri}} + \hat{H}_{\mathrm{SOC}} + \hat{H}_U, \tag{4}$$

where each decomposed part is determined in the following: The hopping terms are given by

$$\hat{H}_0 = \sum_{\ell\neq m} \sum_{a,b=xy,yz,zx} \sum_{\sigma,\sigma'} t^{\sigma\sigma'}_{\ell,m;a,b} [\hat{c}^\dagger_{\ell a\sigma} \hat{c}_{mb\sigma'} + \mathrm{H.c.}]. \tag{5}$$

Here we note that, among all the hoppings, the dominant terms are the nearest-neighbor hoppings $t \simeq t^{\sigma\sigma}_{\ell,m;a,b} \simeq t^{\sigma\sigma}_{\ell,m;b,a}$ that satisfy $(a, b) = (zx, xy)$, (xy, yz), or (yz, zx) with $\langle \ell, m\rangle \in X$, Y, and Z, which is consistent with the original proposal [1] for the Kitaev couplings. The x, y, and z axes are illustrated in Fig. 1.

The on-site atomic part is derived from Eq. (3) with $\ell = m$ and can be described as the contribution from the trigonal distortion (with orbital-dependent chemical potentials) and the atomic part of the spin-orbit coupling by introducing a vector representation $\vec{\hat{c}}^\dagger_\ell = (\hat{c}^\dagger_{\ell yz\uparrow}, \hat{c}^\dagger_{\ell yz\downarrow}, \hat{c}^\dagger_{\ell zx\uparrow}, \hat{c}^\dagger_{\ell zx\downarrow}, \hat{c}^\dagger_{\ell xy\uparrow}, \hat{c}^\dagger_{\ell xy\downarrow})$ as

$$\hat{H}_{\mathrm{tri}} = \sum_\ell \vec{\hat{c}}^\dagger_\ell \begin{bmatrix} -\mu_{yz} & \Delta & \Delta \\ \Delta & -\mu_{zx} & \Delta \\ \Delta & \Delta & -\mu_{xy} \end{bmatrix} \hat{\sigma}_0 \vec{\hat{c}}_\ell \tag{6}$$

and

$$\hat{H}_{\mathrm{SOC}} = \frac{\zeta_{\mathrm{so}}}{2} \sum_\ell \vec{\hat{c}}^\dagger_\ell \begin{bmatrix} 0 & +i\hat{\sigma}_z & -i\hat{\sigma}_y \\ -i\hat{\sigma}_z & 0 & +i\hat{\sigma}_x \\ +i\hat{\sigma}_y & -i\hat{\sigma}_x & 0 \end{bmatrix} \vec{\hat{c}}_\ell. \tag{7}$$

Both the off-diagonal elements of the spin-independent part $\hat{H}_{\rm tri}$ and the spin-dependent part $\hat{H}_{\rm SOC}$ can be well described by a single parameter Δ and $\zeta_{\rm so}$, respectively. Because of the inherent crystal anisotropy differentiating Ir-Ir bonds along the b axis from others [23], the chemical potential for the xy orbitals, μ_{xy}, is different from μ_{yz} and μ_{zx}. The symmetry of these terms is slightly broken in the real crystal due to the stacking fault along the c axis and the locations of other ions. However, the deviation is much smaller than 0.005 eV.

The Coulomb term expressed by the Wannier orbital basis is well described by a symmetric form as

$$\hat{H}_U = U\sum_{\ell}\sum_{a=yz,zx,xy}\hat{n}_{\ell a\uparrow}\hat{n}_{\ell a\downarrow} + \sum_{\ell\neq m}\sum_{a,b}\frac{V_{\ell,m}}{2}\hat{n}_{\ell a}\hat{n}_{mb} + \sum_{\ell}\sum_{a<b}\sum_{\sigma}[U'\hat{n}_{\ell a\sigma}\hat{n}_{\ell b\bar{\sigma}} + (U'-J_{\rm H})\hat{n}_{\ell a\sigma}\hat{n}_{\ell b\sigma}] + J_H\sum_{\ell}\sum_{a\neq b}[\hat{c}^{\dagger}_{\ell a\uparrow}\hat{c}^{\dagger}_{\ell b\downarrow}\hat{c}_{\ell a\downarrow}\hat{c}_{\ell b\uparrow} + \hat{c}^{\dagger}_{\ell a\uparrow}\hat{c}^{\dagger}_{\ell a\downarrow}\hat{c}_{\ell b\downarrow}\hat{c}_{\ell b\uparrow}], \quad (8)$$

with the local intraorbital Coulomb repulsion, U, interorbital Coulomb repulsion, U', the Hund's rule coupling, J_H, the interatomic Coulomb repulsion, $V_{\ell,m}$, and $\hat{n}_{\ell a} = \hat{n}_{\ell a\uparrow} + \hat{n}_{\ell a\downarrow}$. The orbital dependences of U, J_H, and V are negligibly small.

The obtained tight binding parameters are given in Table I. We also list the orbital-averaged values of U, U', J_H, and V obtained by the cRPA. We note that $\Delta = -28$ meV for the t_{2g} model [24]. One might think that $\Delta = -28$ meV looks like a tiny parameter. However, it is crucial to keep it because it generates relevant anisotropy illustrated later in Fig. 3.

Strong coupling limit, minimal spin model for A_2IrO_3.— The *ab initio* parameters for the generalized Kitaev-Heisenberg model (1) are derived from the t_{2g} Hamiltonian $\hat{H}_{t2g}$ in Eq. (4) by the second order perturbation theory: Here we take $\hat{H}_{\rm tri} + \hat{H}_{\rm SOC} + \hat{H}_U$ as an unperturbed Hamiltonian and $\hat{H}_0$ as a perturbation. Since the ground state of $\hat{H}_{\rm tri} + \hat{H}_{\rm SOC} + \hat{H}_U$ is degenerate, we employ the standard degenerate perturbation theory. If we neglect Δ and μ_a ($a = yz, zx, xy$), the lowest Kramers doublets become so-called $J_{\rm eff} = 1/2$ states. The atomic ground state of an isolated iridium atom is preserved to be a doublet irrespective of the amplitudes of Δ [19], whose degeneracy is protected by the time-reversal symmetry. Then the generalized Kitaev-Heisenberg model describing pseudospin degrees of freedom is justified as an effective model in the ground state as well as at a finite temperature unless it exceeds both of Δ and $\zeta_{\rm so}$.

The exchange couplings $\mathcal{J}_Z$, $\mathcal{J}_X$, $\mathcal{J}_Y$, and further neighbor couplings are derived through the second order perturbation theory by numerically diagonalizing the local part of the Hamiltonian $\hat{H}_{\rm tri} + \hat{H}_{\rm SOC} + \hat{H}_U$ and by including all order terms with respect to $\zeta_{\rm so}$ and Δ, irrespective of their amplitudes. (See Supplemental Material [19].) Thus obtained *ab initio* values for Na_2IrO_3 are given in Table II. We remark that $K \sim -30.1$ meV is negative and $J \sim 4.4$ meV is positive for the Z bonds. For numerical calculations, we also include the second and third neighbor couplings for more accurate *ab initio* calculations [19].

The model (1) with the *ab initio* parameters in Table II together with small and detailed second and third neighbor exchange couplings [19] was solved by the exact diagonalization for a 24-site cluster. We also calculate finite temperature properties for the cluster by using the thermal pure quantum states [26], which offer an algorithm similar to the finite-temperature Lanczos [27] and earlier works [28]. They well reproduce the experimentally observed zigzag magnetic order as the ground state and finite temperature properties. See the detailed results in later discussions for Fig. 2 and the Supplemental Material [19].

Neither large further neighbor exchange couplings [7,8,12,13] nor antiferromagnetic Kitaev couplings $K > 0$ [11,30] assumed and required to reproduce the experimental zigzag magnetic order in the literature are realistic in the *ab initio* point of view. In addition, the amplitudes of the anisotropic couplings I_1 and I_2 comparable with J are crucially important to reproduce the experimental results, contrary to the assumptions in Refs. [11] and [30]. The e_g-orbital degrees of freedom, proposed to change the sign of K in Ref. [11] and neglected in the present Letter, generate only minor corrections [19].

The stabilization of the zigzag order is interpreted as follows: If we assume the magnetic ordered moment along $(x, y, z) = (1, 1, 0)$, the zigzag order is interpreted as

TABLE I. One-body and two-body parameters for $\hat{H}_{t2g}$. The most relevant hopping parameter t, the atomic spin-orbit coupling $\zeta_{\rm so}$, and the trigonal distortion Δ, are shown for the one-body part. Here, t is for $t^{\sigma,\sigma}_{\ell,m;\xi,\eta}$ for $\langle\ell, m\rangle$ being the Z bond and its symmetric replacement for X and Y bonds. As for the two-body parameters, we list the cRPA results for the local intraorbital Coulomb repulsion U, the Hund's rule coupling J_H, and the orbital-independent nearest-neighbor Coulomb repulsion V. Other small one-body parameters are given in Ref. [19].

One-body parameters (eV)	t	$\mu_{xy} - \mu_{yz,zx}$	$\zeta_{\rm so}$	Δ
	0.27	0.035	0.39	−0.028
Two-body parameters (eV)	U	U'	J_H	V
	2.72	2.09	0.23	1.1

TABLE II. Nearest-neighbor exchange couplings derived by the strong coupling expansion from the *ab initio* t_{2g} model.

$\mathcal{J}_Z$ (meV)	K	J	I_1	I_2		
	−30.7	4.4	−0.4	1.1		
$\mathcal{J}_{X,Y}$ (meV)	K'	J'	J''	I'_1	I'_2	I''_2
	−23.9	2.0	3.2	1.8	−8.4	−3.1

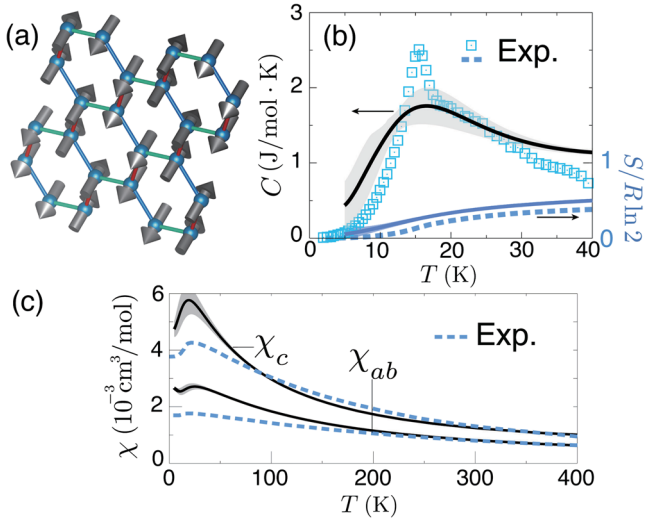

FIG. 2 (color online). Ground state and finite temperature properties of the generalized Kitaev-Heisenberg model for Na_2IrO_3 calculated for the 24-site cluster by using the Lanczos method and thermal pure quantum states [26]. (a) Ground state magnetic order determined by applying tiny local magnetic fields ($\sim 10^{-2}$ meV) at a single site. (b) Temperature dependence of specific heat C and entropy S, which are consistent with an experiment [29]. Shaded area shows uncertainty due to finite size effects [26]. (c) Temperature-dependence of in-plane and out-of-plane magnetic susceptibilities, which are also consistent with the experiment [29] at high temperatures.

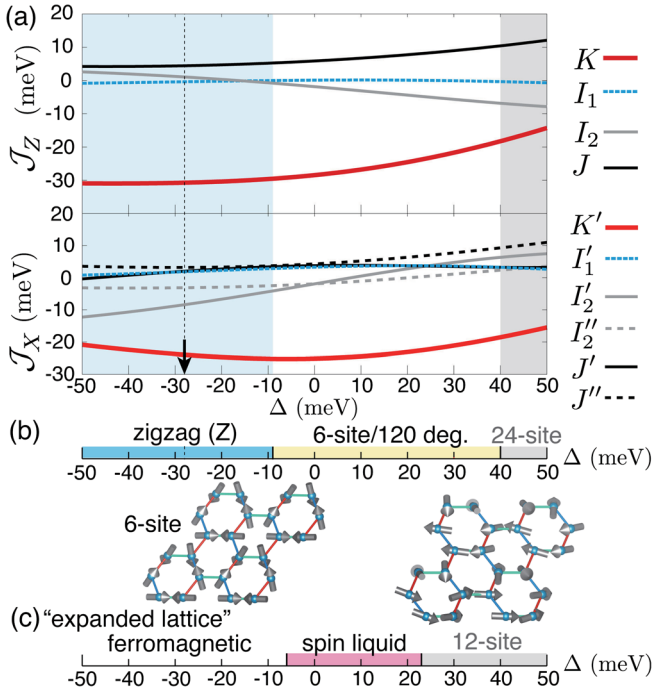

FIG. 3 (color online). (a) Δ dependence of matrix elements of $\mathcal{J}_Z$, $\mathcal{J}_X$ as functions of Δ. Around the *ab initio* values at Δ (~ -28 meV) listed in Table II, $K < 0$, $K' < 0$, $J > 0$, $J' > 0$, and $J'' > 0$ are stably satisfied with gradual dependences on Δ. (b) Ground state phase diagram for Na_2IrO_3 with lattice distortions represented by changes in Δ. The phase boundaries are determined by anomalies (peaks signaling continuous transitions) in second derivatives of the exact energy for the 24-site cluster with respect to Δ. Around the *ab initio* parameter $\Delta = -28$ meV, the zigzag order appears. By increasing Δ, a 6-site unit cell order (or 120° structure [30]) illustrated in the lower left panel and a 24-site unit cell long-period order [19], appear. (c) Δ dependence of the ground state of the generalized Kitaev-Heisenberg model for "expanded lattices." Here we neglect the small hopping parameters other than t and take a larger Hund's rule coupling $J_H = 0.3$ eV. Spin liquid phases compete with ferromagnetic states and 12-site unit cell orders illustrated in the upper right panel [19], where the phase transitions among them are also interpreted as continuous ones.

ferromagnetically ordered chains consisting of the X and Y bonds (stabilized by K' and I''_2), antiferromagnetically coupled to each other by the Z bonds with J, which is in contrast to a quantum-chemistry estimate that neglects I_2, I'_2, and I''_2 [23]. Indeed, these four exchange couplings, $K \sim K' < 0$, $J > 0$, and $I''_2 < 0$, are crucial to reproduce the zigzag order [19]. The alignment along (1,1,0) assumed here indeed agrees with the result of the pinning field analysis [19] shown in Fig. 2(a). It is also confirmed by the nearest-neighbor spin-spin correlations, $\langle \hat{S}^x_\ell \hat{S}^x_m \rangle = \langle \hat{S}^y_\ell \hat{S}^y_m \rangle = -0.021$, $\langle \hat{S}^z_\ell \hat{S}^z_m \rangle = 0.128$, for the Z bond, and $\langle \hat{S}^x_\ell \hat{S}^x_m \rangle = 0.052(0.098)$, $\langle \hat{S}^y_\ell \hat{S}^y_m \rangle = 0.098(0.052)$, $\langle \hat{S}^z_\ell \hat{S}^z_m \rangle = -0.020$, for the X bond (Y bond).

Comparison with experiments.—Our effective spin model reproduces not only the zigzag order but also magnetic specific heat and anisotropic uniform magnetic susceptibilities consistently with experiments, as shown in Fig. 2(b) and 2(c). For the specific heat, our results are consistent without adjustable parameters. The uniform magnetic susceptibilities χ show Curie-Weiss behaviors and $\chi_{ab} < \chi_c$, where χ_{ab} (χ_c) is the inplane (out-of-plane) susceptibility, which are consistent with experiments. If we introduce a g factor, $g = 1.5$, and anisotropic van Vleck term, $\chi_0 = 1 \times 10^{-4}$ cm^3/mol for χ_c, high-temperature behaviors of χ are qualitatively reproduced as shown in Fig. 2(c). Here we note that the electron's spin moments are different from those of the effective spin models depending on the choice of the Kramers doublets, $|\uparrow\rangle$ and $|\downarrow\rangle$ [19]. For the calculation of χ, we project the original Zeeman term to the effective spin basis $\hat{S}^{x,y,z}_\ell$ [19]. It is left for future studies to relate linear spin wave analysis of our model to the inelastic neutron scattering experiment [7].

Phase diagram in lattices distorted from Na_2IrO_3.—Now we examine the sensitivity of the ground state for the *ab initio* parameter of Na_2IrO_3 to perturbations and search candidates of other quantum states possibly induced by a thermodynamic control such as pressure or in derivatives of Na_2IrO_3 such as $Na_{2-x}Li_xIrO_3$ [31]. Here we choose the trigonal distortion Δ as an experimentally accessible control parameter. First, the Δ dependence of the exchange couplings is illustrated in Fig. 3(a), where the parameters of the *ab initio* t_{2g} Hamiltonian other than Δ are kept unchanged, and the exchange couplings are estimated from the same

strong coupling expansion by changing Δ. The ground state of the generalized Kitaev-Heisenberg model with the Δ-dependent exchange couplings is shown in Fig. 3(b).

How to approach spin liquids.—As already evident in Table II, the *ab initio* effective spin model for Na_2IrO_3 is governed by dominant Kitaev-type ferromagnetic exchange couplings. By expanding the lattice, the spin liquid phase may become accessible: Expansion of the lattice makes the hopping parameters other than the dominant one t negligible. In addition, the environment of the iridium atoms approaches the spherical limit where the intraorbital Coulomb repulsion U' satisfies $U' = U - 2J_H$. Indeed, when we omit the hopping parameters other than t and increase J_H up to 0.3 eV to satisfy $U' = U - 2J_H$, we obtain the spin liquid states adiabatically connected to the Kitaev's spin liquid as shown in Fig. 3(c).

Summary.—We have shown that the realistic parameter of the *ab initio* model for Na_2IrO_3 reproduces the experimentally observed robust zigzag magnetic order, while a quantum spin liquid phase adiabatically connected to the Kitaev spin liquid emerges when the smaller trigonal distortion Δ and expanded lattice constants are satisfied. In this sense, uniaxial strain to reduce Δ is helpful as an approach to realize the spin liquids. Clearly further studies are needed: A more accurate estimate of the phase diagram of the generalized Kitaev-Heisenberg model is certainly helpful. More detailed studies by taking account of full quantum fluctuations and the effects of realistic itinerancy beyond the strong coupling limit are future intriguing issues.

The authors thank Tsuyoshi Okubo for sharing his unpublished data. Y. N. is supported by the Grant-in-Aid for JSPS Fellows (Grant No. 12J08652). M. K. is supported by Grant-in-Aid for JSPS Fellows (Grant No. 12J07338). R. A. is supported by Funding Program for World-Leading Innovative R&D on Science and Technology (FIRST program) on "Quantum Science on Strong Correlation." This work is financially supported by MEXT HPCI Strategic Programs for Innovative Research (SPIRE) (hp130007) and Computational Materials Science Initiative (CMSI). Numerical calculation was partly carried out at the Supercomputer Center, Institute for Solid State Physics, University of Tokyo. This work was also supported by Grant-in-Aid for Scientific Research (No. 22104010 and No. 223400901) from MEXT, Japan.

[1] G. Jackeli and G. Khaliullin, Phys. Rev. Lett. **102**, 017205 (2009).
[2] J. Chaloupka, G. Jackeli, and G. Khaliullin, Phys. Rev. Lett. **105**, 027204 (2010).
[3] X. Wan, A. M. Turner, A. Vishwanath, and S. Y. Savrasov, Phys. Rev. B **83**, 205101 (2011).
[4] W. Witczak-Krempa, C. Gang, Y.-B. Kim, and L. Balents, Annu. Rev. Condens. Matter Phys. **5**, 57 (2014).
[5] A. Kitaev, Ann. Phys. (Amsterdam) **321**, 2 (2006).
[6] R. Comin *et al.*, Phys. Rev. Lett. **109**, 266406 (2012).
[7] S. K. Choi *et al.*, Phys. Rev. Lett. **108**, 127204 (2012).
[8] F. Ye, S. Chi, H. Cao, B. C. Chakoumakos, J. A. Fernandez-Baca, R. Custelcean, T. F. Qi, O. B. Korneta, and G. Cao, Phys. Rev. B **85**, 180403 (2012).
[9] Y. Singh, S. Manni, J. Reuther, T. Berlijn, R. Thomale, W. Ku, S. Trebst, and P. Gegenwart, Phys. Rev. Lett. **108**, 127203 (2012).
[10] J. Reuther, R. Thomale, and S. Trebst, Phys. Rev. B **84**, 100406 (2011).
[11] J. Chaloupka, G. Jackeli, and G. Khaliullin, Phys. Rev. Lett. **110**, 097204 (2013).
[12] I. Kimchi and Y.-Z. You, Phys. Rev. B **84**, 180407 (2011).
[13] A. F. Albuquerque, D. Schwandt, B. Hetényi, S. Capponi, M. Mambrini, and A. M. Läuchli, Phys. Rev. B **84**, 024406 (2011).
[14] S. Bhattacharjee, S.-S. Lee, and Y. B. Kim, New J. Phys. **14**, 073015 (2012).
[15] I. I. Mazin, H. O. Jeschke, K. Foyevtsova, R. Valentí, and D. I. Khomskii, Phys. Rev. Lett. **109**, 197201 (2012).
[16] T. Miyake and M. Imada, J. Phys. Soc. Jpn. **79**, 112001 (2010).
[17] http://elk.sorceforge.net/.
[18] J. P. Perdew and Y. Wang, Phys. Rev. B **45**, 13244 (1992).
[19] See Supplemental Material at http://link.aps.org/supplemental/10.1103/PhysRevLett.113.107201 for the details of the DFT electronic structures, the atomic ground states, relationship between physical and effective spins, further neighbor couplings, and numerical identification of magnetic orders.
[20] R. Arita, J. Kuneš, A. V. Kozhevnikov, A. G. Eguiluz, and M. Imada, Phys. Rev. Lett. **108**, 086403 (2012).
[21] F. Aryasetiawan, M. Imada, A. Georges, G. Kotliar, S. Biermann, and A. I. Lichtenstein, Phys. Rev. B **70**, 195104 (2004).
[22] A. Kozhevnikov, A. Eguiluz, and T. Schulthess, in *SC'10: Proceedings of the 2010 ACM/IEEE International Conference for High Performance Computing, Networking, Storage, and Analysis* (IEEE Computer Society, Washington, DC, 2010), p. 1.
[23] V. K. Katukuri, S. Nishimoto, V. Yushankhai, A. Stoyanova, H. Kandpal, C. Sungkyun, R. Coldea, I. Rousochatzakis, L. Hozoi, and J. van den Brink, New J. Phys. **16**, 013056 (2014).
[24] The small amplitude of the trigonal distortion $\Delta = -28$ meV is different from the previous result [25]. The difference originates from the electronic band structures around the Fermi level in Ref. [25] which is different from the result in Ref. [15] and ours. In addition, in Ref. [25], the tight-binding parameter is obtained through fitting the LDA dispersion, while we directly calculate the hopping matrix elements with the t_{2g} Wannier orbitals.
[25] C. H. Kim, H. S. Kim, H. Jeong, H. Jin, and J. Yu, Phys. Rev. Lett. **108**, 106401 (2012).
[26] S. Sugiura and A. Shimizu, Phys. Rev. Lett. **108**, 240401 (2012).
[27] J. Jaklič and P. Prelovšek, Phys. Rev. B **49**, 5065 (1994).
[28] M. Imada and M. Takahashi, J. Phys. Soc. Jpn. **55**, 3354 (1986).
[29] Y. Singh and P. Gegenwart, Phys. Rev. B **82**, 064412 (2010).
[30] J. G. Rau, Eric Kin-Ho Lee, and H.-Y. Kee, Phys. Rev. Lett. **112**, 077204 (2014).
[31] G. Cao, T. F. Qi, L. Li, J. Terzic, V. S. Cao, S. J. Yuan, M. Tovar, G. Murthy, and R. K. Kaul, Phys. Rev. B **88**, 220414 (2013).